NPS-53-79-005

NAVAL POSTGRADUATE SCHOOL
Monterey, California

SMOOTH INTERPOLATION OF LARGE SETS

OF SCATTERED DATA

Richard Franke
Gregory Nielson

Technical Report for Period Jan 79 - Mar 79

ADA083840

DDC FILE COPY

80   5   6 042

NAVAL POSTGRADUATE SCHOOL
Monterey, California

Rear Admiral Tyler F. Dedman   Jack Borsting
Superintendent   Provost

    This report was prepared by:
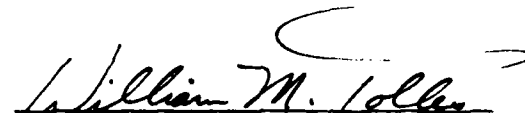
GREGORY NIELSON   RICHARD FRANKE
Associate Professor   Associate Professor
Department of Mathematics   Department of Mathematics
Arizona State University
Tempe, AZ 85281

Reviewed by: Released by:

FRANK D. FAULKNER, Acting Chairman   W. M. TOLLES
Department of Mathematics   Dean of Research

REPORT DOCUMENTATION PAGE	READ INSTRUCTIONS BEFORE COMPLETING FORM
1. REPORT NUMBER NPS-53-79-005 2. GOVT ACCESSION NO. AD-AC83840	3. RECIPIENT'S CATALOG NUMBER
4. TITLE *(and Subtitle)* Smooth Interpolation of Large Sets of Scattered Data	5. TYPE OF REPORT & PERIOD COVERED Technical Report. Jan 1979-Mar 1979 6. PERFORMING ORG. REPORT NUMBER
7. AUTHOR(s) Richard Franke Greg Nielson	8. CONTRACT OR GRANT NUMBER(s) RR 000
9. PERFORMING ORGANIZATION NAME AND ADDRESS Foundation Research Program Naval Postgraduate School - Monterey, CA 93940	10. PROGRAM ELEMENT, PROJECT, TASK AREA & WORK UNIT NUMBERS 61152N, RR 000-01-01 N0001479WR90027
11. CONTROLLING OFFICE NAME AND ADDRESS Chief of Naval Research Arlington, VA 22217	12. REPORT DATE 9 Mar 79 13. NUMBER OF PAGES 36
14. MONITORING AGENCY NAME & ADDRESS*(if different from Controlling Office)*	15. SECURITY CLASS. *(of this report)* Unclassified 15a. DECLASSIFICATION/DOWNGRADING SCHEDULE

16. DISTRIBUTION STATEMENT *(of this Report)*

Approved for public release; distribution unlimited

17. DISTRIBUTION STATEMENT *(of the abstract entered in Block 20, if different from Report)*

18. SUPPLEMENTARY NOTES

19. KEY WORDS *(Continue on reverse side if necessary and identify by block number)*
Scattered data interpolation
Interpolation
Smooth interpolation
Bivariate interpolation
Multivariate approximation

20. ABSTRACT *(Continue on reverse side if necessary and identify by block number)*
Methods for solving the following data fitting problems are discussed: Given the data (x_i, y_i, f_i), $i = 1, \ldots, N$ construct a smooth bivariate function S with the property that $S(x_i, y_i) = f_i$, $i = 1, \ldots, N$. Because the desire to fit this type of data is encountered frequently in many areas of scientific applications, an investigation of the available methods for solving

DD $^{\text{FORM}}_{1\ \text{JAN 73}}$ 1473   EDITION OF 1 NOV 65 IS OBSOLETE
S/N 0102-014-6601 |

this problem was undertaken. Several aspects, such as computational efficiency, fitting characteristics and ease of implementation, were analyzed and compared. Within the context of a general purpose method for large sets of data, two of these methods emerged as being generally superior to the others. It is the purpose of this paper to describe these two methods and present examples illustrating their use and application. FORTRAN programs which implement these methods are available upon request.

Accession For

NTIS C...l

DDC TAB

U...... sed

J...............

By

Distribution

Availability Codes

Dist. | Avail and/or special

A

1. Introduction

The purpose of this paper is to describe two methods for constructing smooth bivariate functions which take on given values at scattered points in the plane. Given the data (x_i, y_i, f_i), $i = 1,...,N$, both of these schemes define a smooth bivariate interpolant S with the property that $S(x_i, y_i) = f_i$, $i = 1,...,N$.

In the past several years a number of methods have been proposed (e.g., [1], [3], [6], [7], [8], and [11]), and two survey papers, [2] and [10], have dealt extensively with this topic. The problem of constructing smooth approximations based upon scattered data is encountered frequently in many areas of scientific applications. Common examples are: meteorological information such as rainfall and solar insolation, geographical information such as elevations, geological information such as depths of underground formations, and engineering data such as stress values obtained by finite element analysis. A somewhat less obvious example is given in [10] where it is described how human heart potential is measured at irregularly spaced points as an aid in diagnosing abnormal heart conditions.

Since a number of methods are available for this important problem, a project was undertaken to test and compare as many methods as possible [4]. While the project included both global methods (meaning that $S(x,y)$ is dependent on all data points regardless of their distance from

(x,y)) and local methods (S(x,y) does not depend on data points more than a certain distance from (x,y)), for large sets of data it is necessary to use local methods. During the course of developing and testing variations of previously published schemes we have discovered two which appear to be preferable as general purpose methods. While neither of these methods have appeared in the literature, they are both modifications of previously described techniques. In Section 2, we describe the basic method from which both of our methods derive. In Section 3, we describe the details of the two modifications and in Section 4 we show the results of applying these methods to certain test problems. In Section 5, we discuss some generalizations and ways to fine tune the schemes to suit the particular needs of a user.

2. Inverse Distance Weighted Least Squares Interpolation

It is convenient to consider the data as coming from an underlying function f and to view the interpolation process as an operator applied to this function. That is, $f_i = f(x_i, y_i)$, $i = 1, \ldots, N$ and $S(x,y) = P[f](x,y)$. Let $\rho_i(x,y)$ denote a function with certain properties of a distance function. In particular, we assume that $\rho_i(x_i, y_i) = 0$ and that $1/\rho_i(x_i, y_i)$ is a nonnegative decreasing function as (x,y) "gets further" from (x_i, y_i). For example, the usual Euclidean distance, $d_i(x,y) = \sqrt{(x - x_i)^2 + (y - y_i)^2}$ is one possibility for ρ_i. We denote by ϕ_j, $j = 1, \ldots, m$ a set of basis functions to be used for a least squares approximation.

McLain [7] was the first to consider a family of inverse distance weighted least squares approximations. The general form of these interpolants is

$$(2.1) \qquad P[f](x,y) = \sum_{j=1}^{m} \bar{a}_j(x,y)\phi_j(x,y)$$

where $\bar{a}_j(x,y)$, $j = 1,\ldots,m$ represents the solution of

$$(2.2) \qquad \underset{a_1,\ldots,a_m}{\text{Min}} \sum_{i=1}^{N} \left[\frac{a_1\phi_1(x_i,y_i) + \ldots + a_m\phi_m(x_i,y_i) - f_i}{\rho_i(x,y)} \right]^2$$

for given (x,y). McLain gave results of a number of tests for several choices of basis functions, ϕ_j, and distance functions, ρ_i. The ϕ_j consisted of the low order monomials, $x^k y^\ell$, and ρ_i was taken as d_i, d_i^2, or $d_i e^{\alpha d_i^2}$. The higher power of d_i and the exponential are motivated by the desire to place less importance on distant data than would be accomplished by d_i alone.

The function (2.1) is not defined at any data point, (x_i, y_i), by the above definition. Because the weight for the best least squares approximation $1/\rho_i^2(x,y) \rightarrow \infty$ as $(x,y) \rightarrow (x_i, y_i)$ it is clear that $P[f](x,y) \rightarrow f_i$ as $(x,y) \rightarrow (x_i, y_i)$, else the sum of the squared errors would be unbounded. Thus we obtain a continuous approximation if we define $P[f](x_i, y_i) = f_i$, $i = 1,\ldots,N$. McLain asserts that the interpolants are infinitely differentiable, and upon the assumption of non-singularity of the coefficient matrix for the normal equations

obtained from (2.2), this readily follows.

McLain singled out the case of the bivariate quadratic, $P[f](x,y) = \bar{a}_1 + \bar{a}_2 x + \bar{a}_3 y + \bar{a}_4 x^2 + \bar{a}_5 xy + \bar{a}_6 y^2$, with weight function $\rho_i = d_i e^{\alpha d_i^2}$ as working well for a variety of problems in the sense that small deviations from certain test functions were observed. Additional experimentation [3] has confirmed this, but even so this method has two serious drawbacks: (1) The computational effort required is large since each evaluation requires the solution of a least squares problem, and (2) the method is global, that is, the interpolant depends on all data points regardless of how far away these points are from the point at which the interpolant is being evaluated.

Both of the methods we propose can be viewed as modifications of the above inverse distance weighted least squares interpolant in that they consist of replacing $\bar{a}_j(x,y)$ with an approximation $A[\bar{a}_j](x,y)$ which is computationally more tractable than $\bar{a}_j(x,y)$ itself. We note that as long as

$$A[\bar{a}_j](x_i,y_i) = \bar{a}_j(x_i,y_i), \quad i = 1,\ldots,N,$$

the operator

$$Q[f](x,y) = \sum_{j=1}^{m} A[\bar{a}_j](x,y)\phi_j(x,y)$$

will maintain the interpolatory properties of $P[f]$. The type

of approximation we use for $\bar{a}_j$, $j = 1,\ldots,m$ is of the form

$$A[\bar{a}_j](x,y) = \sum_{i=1}^{N} \bar{a}_j(x_i,y_i) \, W_i(x,y)$$

where

(2.3) $W_i(x_j,y_j) = \delta_{ij}$, $i, j = 1,\ldots,N$.

Therefore, we may rewrite the above expression for Q as

(2.4) $$Q[f](x,y) = \sum_{i=1}^{N} W_i(x,y)Q_i(x,y)$$

where $Q_i(x,y) = \sum_{j=1}^{m} \bar{a}_j(x_i,y_i)\phi_j(x,y)$ is the inverse distance

weighted least squares fit at the point (x_i,y_i).

   We refer to the functions Q_i, $i = 1,\ldots,N$ as the nodal

functions since they are associated with the nodes (x_i,y_i),

$i = 1,\ldots,N$, respectively. We note that $Q_i(x_i,y_i) = f_i$,

$i = 1,\ldots,N$, and that $Q_i(x,y)$ is a local approximation (near

(x_i,y_i)) to $f(x,y)$, and as such may be expected to mimic

the shape of $f(x,y)$ provided distant points do not influence

$Q_i(x,y)$ too much.

   In order for the interpolant $Q[f]$ to maintain the local

shape characteristics of the nodal functions we will require

certain properties for the W_i in addition to (2.3). Specif-

ically, to preserve

$$\frac{\partial Q[f]}{\partial x}(x_i, y_i) = \frac{\partial Q_i}{\partial x}(x_i, y_i)$$

and

$$\frac{\partial Q[f]}{\partial y}(x_i, y_i) = \frac{\partial Q_i}{\partial y}(x_i, y_i), \ i = 1, \ldots, N \ ;$$

we require that

$$(2.5) \qquad \frac{\partial W_i}{\partial x}(x_j, y_j) = \frac{\partial W_i}{\partial y}(x_j, y_j) = 0, \ i, \ j = 1, \ldots, N.$$

For our two methods, we also propose the use of bivariate quadratics for $Q_i(x,y)$, $i = 1, \ldots, N$. Thus, if f itself is a quadratic function, the function Q_i will be identical to f, i.e., $Q_i(x,y) = f(x,y)$, $i = 1, \ldots, N$. Therefore

$$Q[f](x,y) = \sum_{i=1}^{N} W_i(x,y) Q_i(x,y) = f(x,y) \sum_{i=1}^{N} W_i(x,y)$$

whenever f is a quadratic function. In order to obtain quadratic precision of the modified interpolant $Q[f]$, we add the additional requirement that

$$(2.6) \qquad \sum_{i=1}^{N} W_i(x,y) \equiv 1.$$

The choice of the distance function to be used in (2.2) when calculating the nodal functions was made on the basis

of extensive numerical testing [4].   Franke and Little [2,

p. 112] proposed

$$(2.7) \qquad \frac{1}{\rho_i} = \frac{(R_i - d_i)_+}{R_i d_i} \quad , \quad (R_i - d_i)_+ = \begin{cases} R_i - d_i \ , & R_i - d_i \ge 0 \\ 0 & R_i - d_i < 0 \end{cases} ,$$

and for appropriate choice of the values R_i , this works well.

We recall that Q_k is the solution of the inverse distance weighted

least squares problem at $(x,y) = (x_k, y_k)$.   Discussion of the Q_k

is simplified (as is the actual computation) by assuming

that

$$Q_k(x,y) = f_k + \bar{a}_{k2}(x-x_k) + \bar{a}_{k3}(y-y_k) + \bar{a}_{k4}(x-x_k)^2 +$$

$$\bar{a}_{k5}(x-x_k)(y-y_k) + \bar{a}_{k6}(y-y_k)^2 \quad .$$

We then seek the solution of

$$\underset{a_{k2}, \ldots, a_{k6}}{\text{Min}} \quad \sum_{\substack{i=1 \\ i \ne k}}^{N} \left[\frac{f_k + a_{k2}(x_i-x_k) + \ldots + a_{k6}(y_i-y_k)^2 - f_i}{\rho_i(x_k, y_k)} \right]^2 \quad .$$

If $\frac{1}{\rho_i}$ is given by (2.7), then whenever $d_i(x_k, y_k) > R_i$,

the point (x_i, y_i, f_i) has no influence since the corresponding

term in the sum is zero.   Thus Q_k depends only on "nearby"

points and is therefore a local approximation to f.   If we now

use weight functions W_k which are nonzero only in some neigh-

borhood of (x_k, y_k) we will obtain a local interpolant.

The proper choice of the "radii of influence", R_i,

is critical to the success of the method, and we will discuss

this in the context of our first method in the next section, as well as in Section 5.

3. Two Methods for Interpolation To Scattered Data

Specifying the weight functions $W_i(x,y)$, $i = 1,...,N$ to be used in (2.4) will define an interpolant. We have found that both of the choices we propose have very comparable fitting capabilities, but we feel that there are situations in which one or the other may be preferable, and so both are presented.

3.1 Method I.

This scheme is based upon a special case of the inverse distance weighted least squares interpolant given by (2.1) - (2.2). If $m = 1$ and $\phi_1(x) \equiv 1$, then (2.2) can be explicitly solved to yield

$$\bar{a}_1(x,y) = \frac{\sum_{i=1}^{N} \frac{f_i}{\rho_i^2}(x,y)}{\sum_{i=1}^{N} \frac{1}{\rho_i^2}(x,y)}$$

and so

$$(3.1) \qquad P[f] = \frac{\sum_{i=1}^{N} \frac{f_i}{\rho_i^2}}{\sum_{i=1}^{N} \frac{1}{\rho_i^2}}$$

This method was first proposed by Shepard [11]. Without modification it does not have very good fitting properties. Gordon and Wixom [5] have analyzed this method and have proposed some interesting modifications. They also discuss some application areas that are well suited for this type of interpolant. The fact that Shepard's method is a special case of inverse distance weighted least squares interpolants has been pointed out by several authors, e.g. [10]. It can easily be verified that as long as $\rho_i(x_i, y_i) = 0$, the functions

$$(3.2) \qquad W_i = \frac{\dfrac{1}{\rho_i^2}}{\displaystyle\sum_{k=1}^{N} \frac{1}{\rho_k^2}}$$

will satisfy the conditions of (2.3), (2.5), and (2.6). This last statement assumes that the distance functions ρ_i, $i = 1,\ldots,N$ are sufficiently smooth so that the derivatives (2.5) exist. This is certainly the case for our choice of ρ_i, $i = 1,\ldots,N$ given by (2.7).

We complete the description of our first method with a discussion of the selection of the R_i involved in the definition of ρ_i. While the use of variable radii (i.e., $R_i \neq R_j$) adds to the flexibility of the methods, we have found that for a general purpose interpolant, the selection of these values can quite often be a nuisance which can be avoided by the use of a uniform value ($R_i = R$ for all i).

At this point we emphasize that the distance functions ρ_i enters in two places: (1) definition of the nodal

functions, Q_k, and (2) definition of the weight functions, W_k.
It is not necessary to use the same radius of influence for
both instances, and experience has shown it is desirable to use
different values, say $R = R_q$ in defining the nodal functions,
and $R = R_w$ in defining the weight functions. Since R_q denotes
the radius of influence of the data points on the nodal functions,
while R_w denotes the radius of influence of the nodal functions
on the interpolant $Q[f](x,y)$, it is clear we should take $R_w \leq$
R_q. In order to aid the naive user in making reasonable choices
of R_q and R_w we have found it convenient to specify values of
N_q and N_w and to compute the radii of the influence regions
according to the relationships:

$$R_q = \frac{D}{2} \sqrt{\frac{N_q}{N}}$$

(3.3)

$$R_w = \frac{D}{2} \sqrt{\frac{N_w}{N}}$$

where $D = \max_{i,j} d_i(x_j, y_j)$.

These choices of R_q and R_w eliminate the effects of scaling
the data. The values of N_q and N_w can be thought of as
representing the number of data points anticipated to lie in
circles of radii R_q and R_w, respectively. For somewhat uniformly
distributed data, we have found that a value of $N_q = 18$ works
quite well. For data that have some regions which are
relatively sparsely populated and other regions where the
data are comparatively dense, or for small sets ($N < 25$), it
may be necessary to increase the values, since the interpolant

is defined only on the union of disks of radius R_w centered
at the data points (x_i, y_i), $i = 1, \ldots, N$. We have also found
that the use of the relationship $N_q/N_w \sim 2$ is useful. To
avoid problems when fewer than five additional data points
fall within a distance R_q of some given (x_i, y_i), we have
incorporated an automatic fallback to linear nodal functions
in this case. In general, we use the singular value decomposi-
tion to compute the coefficients of the nodal functions, which
avoids possible nonuniqueness problems. It is not usual for
either situation to occur, however.

We now summarize the description of our first method.

i) Select N_q and N_w in order to define

$$\frac{1}{\rho_i} = \frac{(R_q - d_i)_+}{R_q d_i} \quad , \quad R_q = \frac{D}{2} \sqrt{\frac{N_q}{N}}$$

$$\frac{1}{\bar{\rho}_i} = \frac{(R_w - d_i)_+}{R_w d_i} \quad , \quad R_w = \frac{D}{2} \sqrt{\frac{N_w}{N}}$$

Default values of N_q and N_w are 18 and 9, respectively.

ii) For $k = 1, \ldots, N$ solve the least squares problem:

$$\min_{a_{kj}, j=2,\ldots,6} \sum_{\substack{i=1 \\ i \neq k}}^{N} \frac{1}{\rho_i^2(x_k, y_k)} \left[f_k + a_{k2}(x_i - x_k) + a_{k3}(y_i - y_k) \right.$$

$$\left. + a_{k4}(x_i - x_k)^2 + a_{k5}(x_i - x_k)(y_i - y_k) + a_{k6}(y_i - y_k)^2 - f_i \right]^2$$

to yield $\bar{a}_{kj}$, $j = 2,\ldots,6$.

    iii) Define

$$Q_k(x,y) = f_k + \bar{a}_{k2}(x-x_k) + \bar{a}_{k3}(y-y_k)$$

$$+ \bar{a}_{k4}(x-x_k)^2 + \bar{a}_{k5}(x-x_k)(y-y_k) + \bar{a}_{k6}(y-y_k)^2$$

and compute

$$D[f](x,y) = \frac{\displaystyle\sum_{k=1}^{N} \frac{Q_k(x,y)}{\hat{\rho}_k^2(x,y)}}{\displaystyle\sum_{k=1}^{N} \frac{1}{\hat{\rho}_k^2(x,y)}}$$

3.2   Method II.

Our second method makes use of a triangulation of the data $V_i = (x_i, y_i)$ $i = 1,\ldots,N$ in order to define the weight functions W_i, $i = 1,\ldots,N$. We use an algorithm which triangulates the convex hull based upon the min-max angle criterion as described by Lawson [6]. A FORTRAN program which implements this algorithm is available as part of [1]. Alternatively, if a triangulation is in existence for other purposes, it can be used.

Each W_i will be a globally defined C^1 function with support $S_i = \bigcup_{jkl \,\epsilon\, M_i} T_{jkl}$, where T_{jkl} denotes the triangle with vertices V_j, V_k, and V_l and $M_i = \{jkl: T_{jkl}$ is a triangle with vertex $V_i\}$.
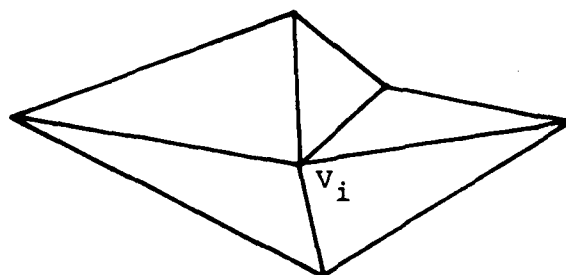
Figure 1: S_i

We first define W_i and its first order partial derivatives on

$E = \underset{kj \in N_e}{U} e_{kj}$ where e_{kj} represents the edge with vertices

V_k and V_j and $N_e = \{kj: \overline{V_k V_j}$ is an edge of the triangulation$\}$.

Following this, we incorporate a blending method for triangles

to extend the definition to the interior of each triangle of

the triangulation. Let e_{ij} be an edge contained in S_i with

V_i as an endpoint. As a univariate function along this edge,

W_i must satisfy four conditions imposed by (2.3) and (2.5).

Namely

$$W_i(V_i) = 1, \quad W_i(V_j) = 0,$$

$$(x_j - x_i)\frac{\partial W_i}{\partial x}(V_i) + (y_j - y_i)\frac{\partial W_i}{\partial y}(V_i) = 0$$

and

$$(x_j - x_i)\frac{\partial W_i}{\partial x}(V_j) + (y_j - y_i)\frac{\partial W_i}{\partial y}(V_j) = 0.$$

These conditions can be satisfied by a cubic polynomial and so we define

$$W_i((1-t)V_i + tV_j) = (1-t)^2(2t+1), \quad 0 \leq t \leq 1.$$

On all other edges we define W_i to be zero. In order to maintain continuity of the first order derivatives across edges, it is convenient to specify the derivatives normal to an edge as a linear function along the edge. That is

$$(y_j-y_i)\frac{\partial W_i}{\partial x}((1-t)V_i + tV_j) - (x_j-x_i)\frac{\partial W_i}{\partial y}((1-t)V_i + tV_j)$$

$$= (1-t)[(y_j-y_i)\frac{\partial W_i}{\partial x}(V_i) - (x_j-x_i)\frac{\partial W_i}{\partial y}(V_i)]$$

$$+ t[(y_j-y_i)\frac{\partial W_i}{\partial x}(V_j) - (x_j-x_i)\frac{\partial W_i}{\partial y}(V_j)].$$

In light of (2.5), this means that the normal derivatives will all be identically zero. This completes the description of the edge information for W_i.

In order to extend the definition of W_i to the interior of each triangle, we use an interpolation method [9] which will assume predescribed position and slope on the entire boundary of a triangle domain. After substituting the edge information into this triangular blending method, we find that for $(x,y) \in T_{ijk} \subset S_i$, the weight functions have the form

$$W_i(x,y) = b_i^2(3-2b_i)$$

$$(3.4) \qquad + 3 \ \frac{b_i^2 b_j b_k}{b_i b_j + b_i b_k + b_j b_k} \Bigg\} \ b_j \left[\frac{\|e_i\|^2 + \|e_k\|^2 - \|e_j\|^2}{\|e_k\|^2} \right]$$

$$+ \ b_k \left[\frac{\|e_i\|^2 + \|e_j\|^2 - \|e_k\|^2}{\|e_j\|^2} \right] \Bigg\} \ .$$

where b_i, b_j, b_k are the barycentric coordinates of (x,y) with respect to the triangle T_{ijk} and $\|e_n\|$ $n = i$, j or k represents the length of the edge opposite V_n, $n = i$, j or k. The barycentric (area) coordinates are given by the equations

$$x = b_i x_i + b_j x_j + b_k x_k$$

$$(3.5) \qquad y = b_i y_i + b_j y_j + b_k y_k$$

$$1 = b_i + b_j + b_k \ .$$

We can now note that on an arbitrary triangle T_{ijk} the only weights which are nonzero are W_i, W_j and W_k. Therefore, the final interpolant is given by

$$(3.6) \qquad G[f](x,y) = W_i(x,y)Q_i(x,y) + W_j(x,y)Q_j(x,y)$$

$$+ W_k(x,y)Q_k(x,y) \ , \ (x,y) \ \varepsilon \ T_{ijk}.$$

We also note that $W_i + W_j + W_k = 1$, so that (2.6) is satisfied. We now summarize this method.

    1)   Define the nodal functions Q_k, $k = 1,\ldots,N$ as in Method I,

    ii)   Form a triangulation of the points $V_i = (x_i, y_i)$, $i = 1,\ldots,N$,

    iii)   Given (x,y) determine the vertices V_i, V_j and V_k of the triangle that contains this point and compute $G[f](x,y)$ according to (3.6) using (3.4) and (3.5).

We note that this method is very similar to that proposed by McLain [8]. Our weight functions W_i, i = 1,...,N arise in a natural manner, however, and use of the distance function given in (2.7) is an improvement since it is generally the case that shape characteristics of the nodal functions in relation to f are adversely influenced when global approximations are used.

4. Examples

In order to illustrate the performance of the two methods, we include some examples. These examples are only a few of many upon which our conclusions are based, but are representative of the methods' approximation properties. The first group of examples utilizes ordinates from the function

$$f(x,y) = .75EXP\left[-\frac{(9x-2)^2+(9y-2)^2}{4}\right] + .75EXP\left[-\frac{(9x+1)^2}{49} - \frac{(9y+1)}{10}\right]$$

$$- .2EXP\left[-(9x-4)^2 - (9y-7)^2\right] + .5EXP\left[-\frac{(9x-7)^2+(9y-3)^2}{4}\right].$$

A perspective plot of this surface, viewed from the first quadrant at an angle of 30° from the x-axis is given in figures 3a and 4a. The function was chosen so as to present a variety of behavior in a single surface. The maximum value of the function is approximately 1.22 near the point (.22, .22), while the minimum value is approximately .004 near the point (.47, .78). Three sets of data (x_i, y_i), i = 1,...,N were used.

Set 1: This set consists of 100 points generated by a pseudorandom number generator, one point in each subsquare
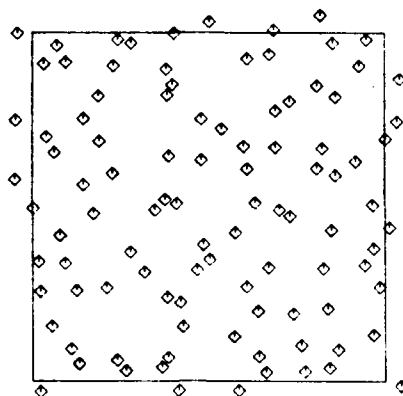
(a) Data Set 1
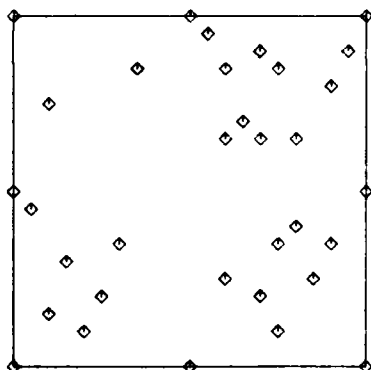
(b) Data Set 2
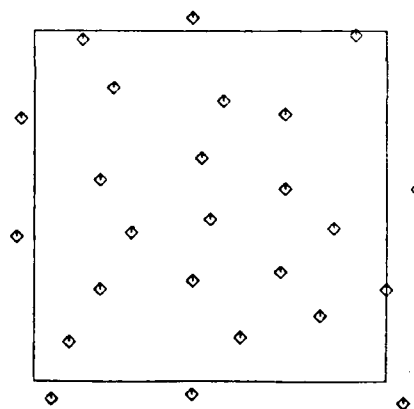
(c) Data Set 3

Figure 2.

of side 1/9 centered at $(i/9, j/9)$, i, $j = 0,1,...,9$. These points are shown in Figure 2a.

Set 2: This set of 33 points was selected manually to have regions of varying density. These points are shown in Figure 2b.

Set 3: This set of 25 points was selected manually to yield a somewhat uniform coverage of the unit square, and are similar to a set appearing in [8]. These points are shown in Figure 2c.

The interpolants were evaluated on a uniform grid of 33 x 33 points in the unit square. The resulting surfaces are shown in Figures 3 and 4. Table 1 contains the maximum, mean, and RMS deviations at these points. For Method II a few of the display points lie outside the convex hull. For plotting purposes, these were set to zero and were omitted in the calculations leading to the errors of Table 1.

| Case	Max	Mean	RMS
I.1	.0573	.0079	.0128
I.2	.1844	.0340	.0478
I.3	.1584	.0353	.0486
II.1	.0481	.0072	.0113
II.2	.1501	.0326	.0455
II.3	.1535	.0349	.0475

Table 1. Errors

Figures 3b and 4b show that both methods reproduce the surface quite well for data set 1. The main defect appears to be near the higher peak, particularly for Method I. As can be seen from the disposition of the points in Figure 2a, this is in a region where a relatively large gap between points occurs. A similar occurrence accounts for the depressed area behind the dip in both figures 3b and 4b.

Figures 3c and 4c are quite similar and both have noticeable defects when compared to the test surface. In particular, the dip is completely missed because the data points fail to define it. The appearance of a crease in Figure 4c near the right rear edge is due to the occurrence of a long thin triangle along that edge which causes blending of two nodal functions from points relatively far apart in the definition of the interpolant for that triangle. When these two nodal functions differ significantly, as they do here, rapid variations can occur across the narrow part of the triangle.

Figures 3d and 4d appear to be less alike than they actually are because values outside the convex hull have been set to zero in Figure 4d. The most significant difference between the two is near the left rear edge, where Figure 3d shows the surface (apparently) dipping down rather rapidly, while Figure 4d shows a near crease similar to that in Figure 4c. Because of a data point near (.47, .78), the dip is partially defined in this case, but since there are no other nearby points it is extended over a much wider area than in the test surface.
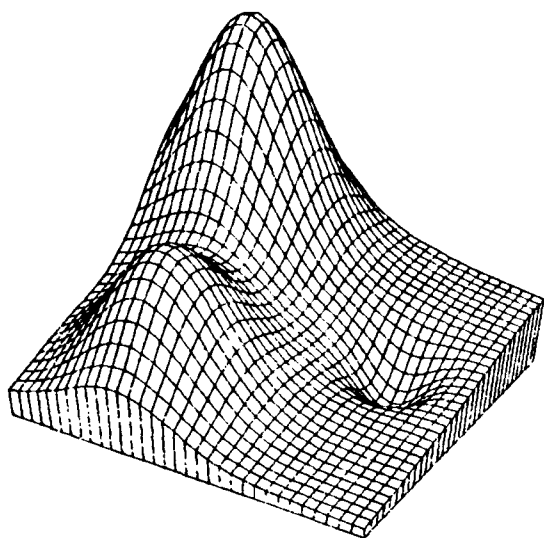
(a) Test surface
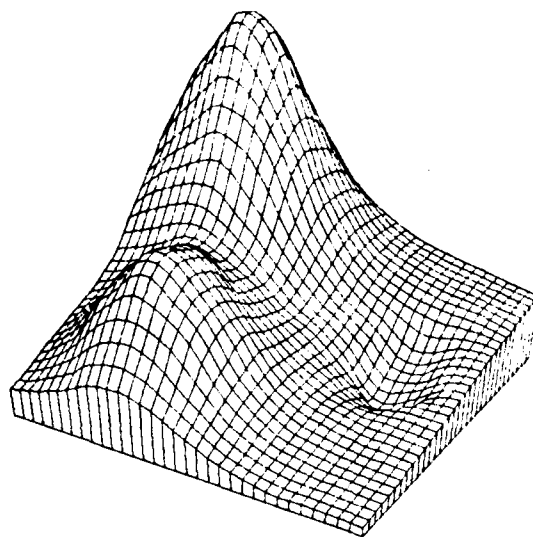
(b) Interpolant for Data Set 1
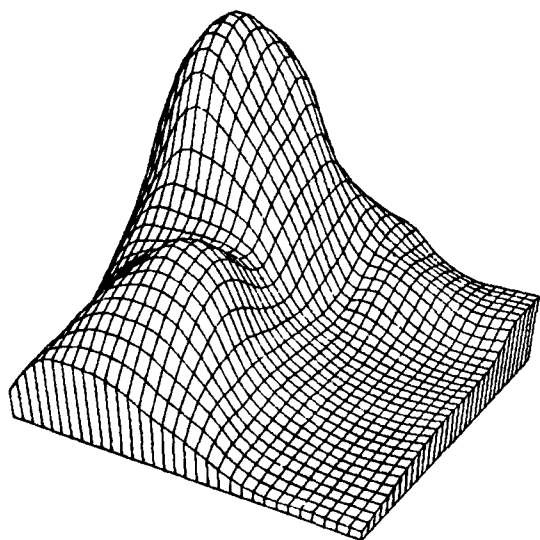
(c) Interpolant for Data Set 2
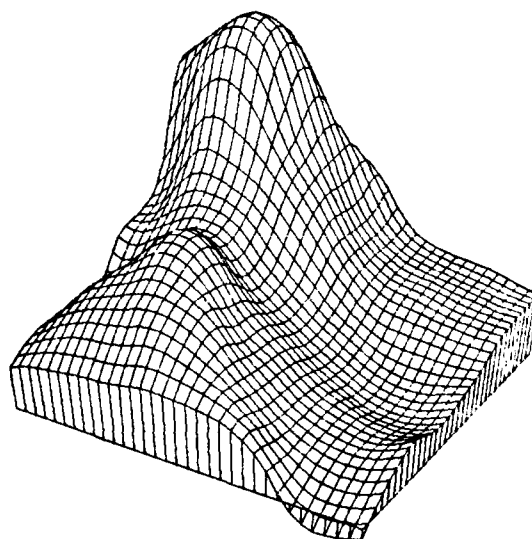
(d) Interpolant for Data Set 3

Figure 3: Method I
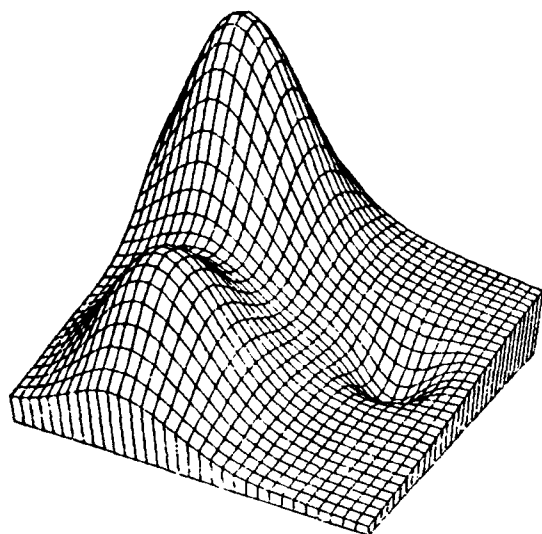
(a) Test surface
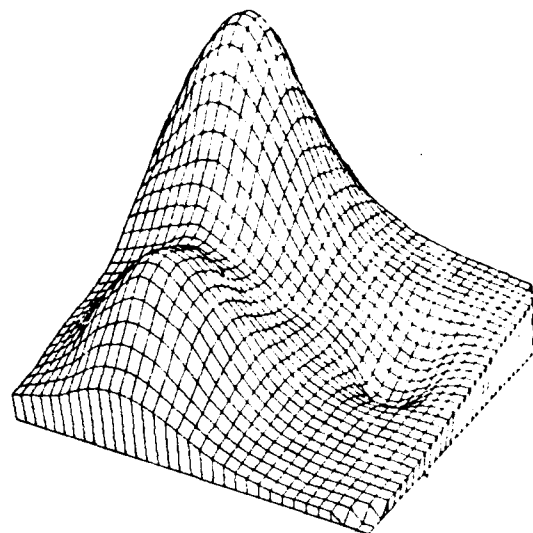
(b) Interpolant for Data Set 1
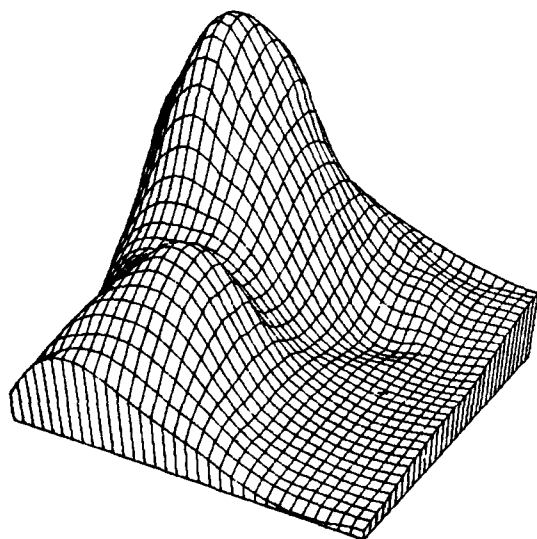
(c) Interpolant for Data Set 2
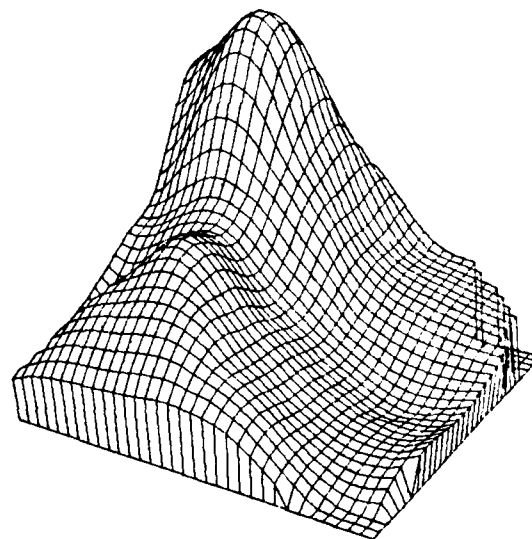
(d) Interpolant for Data Set 3

Figure 4: Method II

Another set of data obtained from Akima [1], which arises in a study of waveform distortion, is given in Table 2. We use this set to illustrate the effects of varying the parameters N_q and N_w. The results are shown in Figure 5.

Figures 5a and 5c appear to be difficult to choose between. Very slight differences can be observed along the front edge. Figure 5e is definitely less desirable than 5a or 5c because of more undulations near the front edge and a higher peak at the right rear. Extensive testing has shown that Method I is fairly stable for values of N_q and N_w in the ranges given here.

Figure 5d appears to be the more desirable surface among 5b, 5d, and 5f. Figure 5b shows a small defect near the right front edge, while the choice between 5d and 5f is less obvious. All three show the characteristic defect over the long slim triangle at the right rear edge, allowing the surface to dip out of sight there. It should be pointed out that there is no known "parent" surface here, and in fact that behavior may be correct, although that part of the interpolant is not pleasing because of the very rapid changes which occur.

5. Conclusions and Recommendations

The two schemes discussed here have been found to be capable of generating reasonable interpolation functions in a variety of cases. A number of comments are appropriate, however.

First, we have restricted ourselves here to the discussion of local interpolants. Local methods are necessary for very large sets of data, but in exploring their properties

i	x_i	y_i	z_i	i	x_i	y_i	z_i
1	11.16	1.24	22.15	26	3.22	16.78	39.93
2	24.20	16.23	2.83	27	0.00	0.00	58.20
3	12.85	3.06	22.11	28	9.66	20.00	4.73
4	19.85	10.72	7.97	29	2.56	3.02	50.55
5	10.35	4.11	22.33	30	5.22	14.66	40.36
6	24.67	2.40	10.25	31	11.77	10.47	13.62
7	19.72	1.39	16.83	32	17.25	19.57	6.43
8	15.91	7.74	15.30	33	15.10	17.19	12.57
9	0.00	20.00	34.60	34	25.00	3.87	8.74
10	20.87	20.00	5.74	35	12.13	10.79	13.71
11	6.71	6.27	30.97	36	25.00	0.00	12.00
12	3.45	12.78	41.24	37	22.33	6.21	10.25
13	19.99	4.62	14.72	38	11.52	8.53	15.74
14	14.26	17.87	10.74	39	14.59	8.71	14.81
15	10.28	15.16	21.59	40	15.20	0.00	21.60
16	4.51	20.00	15.61	41	7.54	10.69	19.31
17	17.43	3.46	18.60	42	5.23	10.72	26.50
18	22.80	12.39	5.47	43	17.32	13.78	12.11
19	0.00	4.48	61.77	44	2.14	15.03	53.10
20	7.58	1.98	29.87	45	0.51	8.37	49.43
21	16.70	19.65	6.31	46	22.69	19.63	3.25
22	6.08	4.58	35.74	47	25.00	20.00	0.60
23	1.99	5.60	51.81	48	5.47	17.13	28.63
24	25.00	11.87	4.40	49	21.67	14.36	5.52
25	14.90	3.12	21.70	50	3.31	0.13	44.08

Table 2.
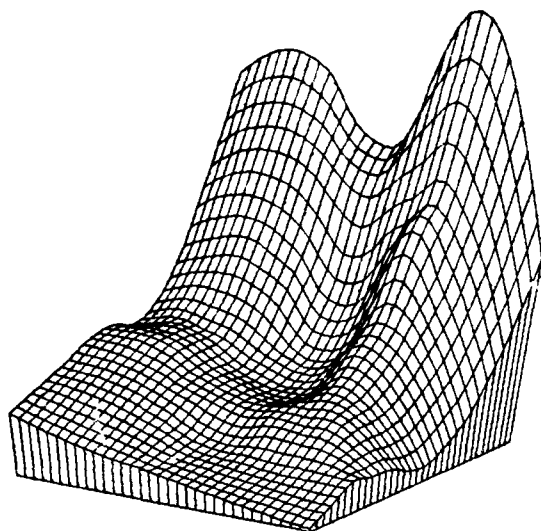
(a) Method I: $N_q=12, N_w=6$
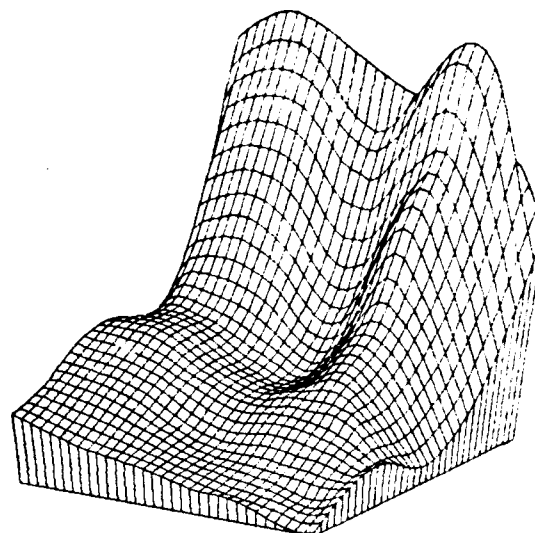
(b) Method II: $N_q=12$
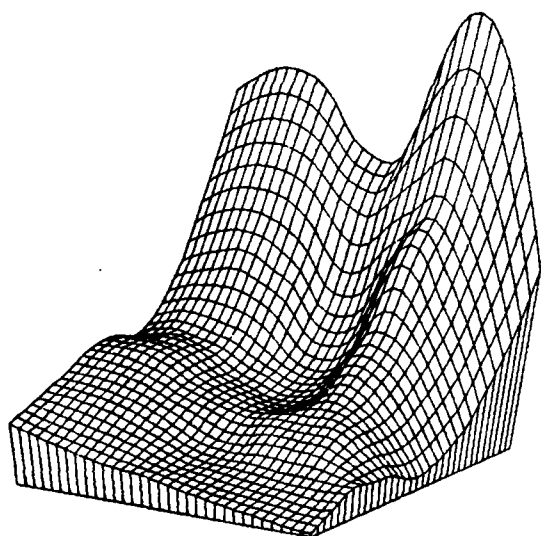
(c) Method I: $N_q=18, N_w=9$
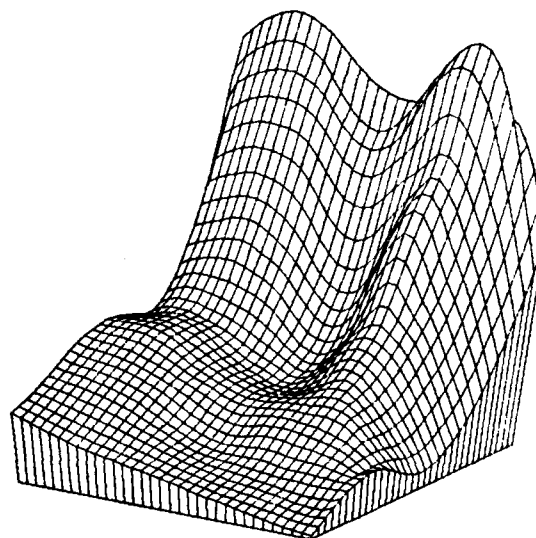
(d) Method II: $N_q=18$

Figure 5.
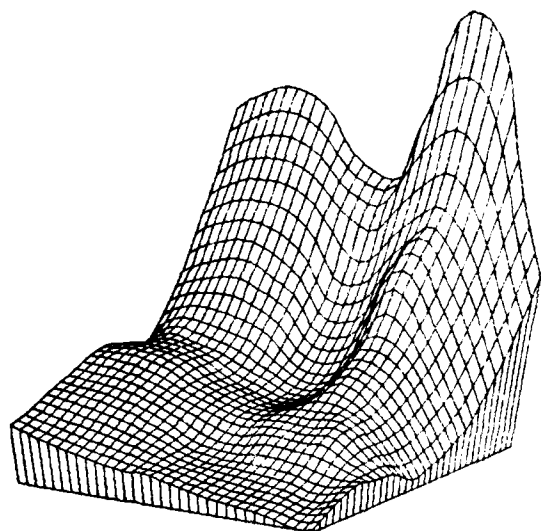
(e) Method I: $N_q=24, N_w=12$
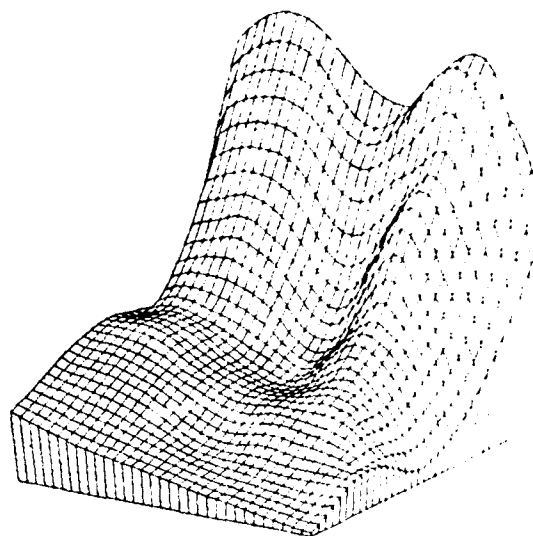
(f) Method II: N_q 24

Figure 5. (continued)

one need not consider large sets because they are local.
We have only considered interpolation methods here, although
we recognize that often it may be more appropriate to use
approximation methods which smooth the data in some sense.
While we have not investigated this possibility, it is clear
that replacement of the nodal functions $Q_k(x,y)$ with local
smoothing functions rather than ones which take on the value
f_k will lead to a smoothing approximation which is local.

The use of the same radius of influence for each point,
and the calculation of that radius from the diameter of the
point set is strictly a matter of convenience for the user.
One could argue that this device makes the methods global
since addition of a point will change the radius of influence
and hence the entire interpolant. For this reason we made the
computation of the radius of influence an option (although
it is the default option). The use of different radii of
influence could be a necessary and desirable feature when the
density of points varies drastically over the point set. Our
experience indicates that one should probably choose radii so
that the disks associated with a point contain approximately 18
points for defining the nodal functions (Methods I and II) and
about 9 points for defining the weight functions (Method I).

Regarding the choice between Method I and Method II,
we make the following comments: Method I has the advantage of
simplicity. While Method II requires a triangulation (and the
machinery for generating it if it is not already available),

and thus more auxiliary storage, it is considerably faster
since each evaluation involves only three nodal functions,
while Method I typically involves about 9 (N_w = 9) nodal
functions. Method II also has the disadvantages noted in
the examples when long thin triangles occur. Method II is
not readily extended to more than two independent variables,
as is Method I. Nonetheless, for certain applications, Method
II may be the appropriate choice, particularly if a triangula-
tion is already in existence.

In conclusion, we note that all local methods involve
some ad hoc assumptions and/or parameters to be specified
by the user. The methods we propose have endured through
extensive testing of their fitting properties and appropriate
values for their parameters. We feel they will perform quite
adequately in a variety of situations. Nonetheless, we
recognize that selection of a suitable interpolant is a sub-
jective matter even in the case of one independent variable,
and thus the choice of an interpolant ultimately rests with the
user.

FORTRAN programs which implement Methods I and II are
available on request from the authors.

References

1. Akima, H., "A method of bivariate interpolation and smooth surface fitting for irregularly distributed data points," ACM TOMS 4(1978) 144-159, and "Algorithm 526: Bivariate interpolation and smooth fitting for irregularly distributed data points," ACM TOMS 4(1978) 160-164.

2. Barnhill, R. E., "Representation and approximation of surfaces," in Mathematical Software III, John R. Rice, ed., Academic Press, New York, 1977, pp. 69-120.

3. Franke, R., "Locally determined smooth interpolation at irregularly spaced points in several variables," JIMA 19(1977) 471-482.

4. Franke, R., "A critical comparison of some methods for interpolation of scattered data," Naval Postgraduate School Technical Report, NPS53-79-003, 1979.

5. Gordon, W. J. and Wixom, J., "On Shepard's method of metric interpolation to bivariate and multivariate data," Mathematics of Computation 32(1978) 253-264.

6. Lawson, C. L., "Software for C^1 surface interpolation," in Mathematical Software III, John R. Rice, ed., Academic Press, New York, 1977, pp. 161-194.

7. McLain, D. H., "Drawing contours from arbitrary data points," The Computer Journal, 17(1974) 318-324.

8. McLain, D. H., "Two dimensional interpolation from random data," The Computer Journal 19, (1976) 178-181, and Errata, The Computer Journal 19, (1976) 384.

9. Nielson, G., "Minimum norm interpolation in triangles," To appear in SIAM Journal on Numerical Analysis.

10. Schumaker, L. L., "Fitting surfaces to scattered data," in Approximation Theory II, edited by G. G. Lorentz, C. K. Chui, and L. L. Schumaker, Academic Press, 1976, pp. 203-268.

11. Shepard, D., "A two dimensional interpolation function for irregularly spaced data," Proc. 23rd Nat. Conf. ACM (1968) 517-523.

DISTRIBUTION LIST

Defense Technical Information Center   2
Cameron Station
Alexandria, VA   22314

Dudley Knox Library   2
Naval Postgraduate School
Monterey, CA   93940

Dean of Research   2
Naval Postgraduate School
Monterey, CA   93940

Department of Mathematics
C. O. Wilde, Chairman   1
F. D. Faulkner, Acting Chairman   1
Professor A. Schoenstadt   1
Professor R. Franke   10
Naval Postgraduate School
Monterey, CA   93940

Dr. Richard Lau   1
Office of Naval Research
1030 East Green St.
Pasadena, CA   91106

Professor R. E. Barnhill   1
Department of Mathematics
University of Utah
Salt Lake City, UT   84112

Professor G. M. Nielson   10
Department of Mathematics
Arizona State University
Tempe, AZ   85281

Chief of Naval Research   2
ATT: Mathematics Program
Arlington, VA   22217

Rosemary E. Chang   1
Sandia Laboratories
Applied Mathematics, Division 2-8235
Livermore, CA   94550

Hiroshi Akima   1
Office of Telecommunications
Department of Commerce
Boulder, CO   80302

Director   6
Naval Research Laboratory
Department of the Navy
4555 Overlook Avenue, S.W.
Washington, D.C. 20375
ATTN: Tech. Information Officer

Director   1
Office of Naval Research/Branch Office
495 Summer Street
Boston, MA 02210

Office of Naval Research   1
New York Area Office
715 Broadway - 5th floor
New York, NY 10003

Director   1
Office of Naval Research/Branch Office
536 South Clark Street
Chicago, IL 60605

Office of Naval Research   1
San Francisco Area Office
760 Market Street - Room 447
San Francisco, CA 94102

Director   6
Naval Research Laboratory
Library, Code 2620
4555 Overlook Avenue, S.W.
Washington, D.C. 20375

Stanford University   1
Department of Mathematics
Stanford, CA 94305

Courant Institute of   1
 Mathematical Sciences
New York University
New York, NY 10012

Massachusetts Institute of Technology   1
Department of Mathematics
Cambridge, MA 02139

Dr. J. A. DeSanto   1
Naval Research Laboratory
Code 8340
Washington, D.C. 20375

Dr. Larry Stedman   1
Naval Ship Research and
 Development Center
Code 1850
Bethesda, MD   20034

Dr. Thomas Corin   1
Naval Ship Research and
 Development Center
Code 1850
Bethesda, MD   20034

Dr. Robert Buchal   1
Naval Research Laboratory
Acoustic Environmental Support
 Detachment
Washington, D.C.   20375

Dr. J. W. Enig   1
Naval Surface Weapons Center
Mathematics Department
White Oak
Silver Spring, MD   20910

Dr. Bruce J. McDonald   1
Office of Naval Research
Code 436, Room 607
Arlington, VA   22217

Mr. Allen L. Hankinson   1
Naval Ship Research and
 Development Center
Code 1833
Bethesda, MD   20034

Charles Micchelli   1
Thomas J. Watson Research Center
P. O. Box 218
Yorktown Heights, NY   10598

Michael Minkoff   1
Applied Mathematics Division
Argonne National Laboratory
9700 South Cass Avenue
Argonne, IL   60439

R. K. Rew   1
NCAR
P. O. Box 3000
Boulder, CO   80307

W. Fichtner   1
Bell Laboratories
Murray Hill, NJ   07974

Peter R. Eiseman
ICASE
MS 132C
NASA Langley Research Center
Hampton, VA 23665   1

Stephen C. Banks
Sun Production Co.   1
503 N. Central Expressway
Richardson, TX 75080

Pablo Barrera
Facultao de Ciencias   1
Dept. de Matematicas
U. N. A. M.
Mexico 20, D. F.
MEXICO

Richard A. Hansen
308 TMCB   1
Brigham Young University
Provo, UT 84601

P. H. Merz
Chevron Research Co.   1
P. O. Box 1627
Richmond, CA 94802

C. Birch
P. O. Box 1267   1
Conoco R & D
Ponca City, OK 74601

James Lyness
AMD-ANL   1
Argonne, IL 60439

Fred N. Fritsch
Lawrence Livermore Laboratories   1
P. O. Box 808 (L-300)
Livermore, CA 94500

W. J. Schaffers
Dupont Co., Engineering Department   1
Exp. Station, 304
Wilmington, DE 19898

U. Ascher
Department of Computer Science   1
University of British Columbia
Vancouver, BC, CANADA

Joe McGrath   1
KMS Fusion, Inc.
3941 Research Park Dr.
Ann Arbor, MI   48104

P. S. Jensen   1
Lockheed Research 5233/205
3251 Hanover St.
Palo Alto, CA   94304

Myron Ginsberg   1
Computer Science Department
General Motors Research Laboratory
Warren, MI   48090

L. Kratz   1
Mathematics Department
Idaho State University
Pocatello, ID   83209

Alan Pierce   1
Amoco Production Co.
P. O. Box 591
Tulsa, OK   74102

A. K. Cline   1
Department of Computer Science
University of Texas at Austin
Austin, TX   78712

W. Roy Wessel   1
CDC
7995 E. Prentice Ave.
Englewood, CO   80111

J. W. Chalmers   1
HAO/NCAR
Box 3000
Boulder, CO   80307

Richard B. Evans   1
Ocean Data Systems, Inc.
6000 Executive Blvd.
Rockville, MD   20852

L. H. Seitelman   1
Pratt and Whitney Aircraft
400 Main Street
East Hartford, CT   06108

John A. Carpenter   1
Oak Ridge National Laboratories
Bldg. 4500-N
Room E208
P. O. Box X
Oak Ridge, TN   37830